



Photonic phase correctors based on phase shifters and grating coupler arrays

Momen Diab^a, Ross Cheriton^b, Jacob Taylor^a, Dhwanil Patel^a, Libertad Rojas^a, Mark Barnet^a, Suresh Sivanandam^{a,c}, Dan-xia Xu^b, Jens H. Schmid^b, Pavel Cheben^b, and Siegfried Janz^b

^aDunlap Institute for Astronomy and Astrophysics, University of Toronto,
Toronto, Ontario, Canada

^bAdvanced Electronics and Photonics Research Centre, National Research
Council Canada, Ottawa, Ontario, Canada

^cDavid A. Dunlap Department of Astronomy and Astrophysics, University of
Toronto, Toronto, Ontario, Canada

ABSTRACT

We propose an integrated phase corrector that efficiently couples the light distorted by atmospheric turbulence into single-mode fibers for the use of free-space optical communication and photonic spectrographs. The integrated circuit consists of an array of gratings that couple light from the subapertures of the telescope pupil into single-mode waveguides in the photonic integrated circuit (PIC). Resistive elements are used to modulate the refractive index in a coiled segment of the waveguides and shift their phases accordingly. The co-phased beams are combined and delivered to an output single-mode fiber (SMF), where the collected flux is predicted to be greater than that coupled directly without correction into a single-mode fiber at the focus of the telescope.

Keywords: Astrophotonics, adaptive optics, phase correctors, photonic spectrograph, free-space optical communication

1. INTRODUCTION

Astrophotonics is driving the transition from conventional bulk optics to integrated optical devices in infrared astronomical instrumentation, where miniaturization simplifies cryogenic control and enables multiplexing. Photonic spectrographs [11], beam combiners [7, 8], wavefront sensors [4], frequency combs [10], and OH suppression filters [6] have been reported in the literature with many undergoing on-sky testing and some becoming facility instruments.

Further author information: (Send correspondence to M.D.)

M.D.: E-mail: momen.diab@utoronto.ca

Turbulence-induced distortions in light waves propagating through Earth’s atmosphere limit the ability to couple them into single-mode fibers (SMFs) which is necessary for most photonic devices. These temporal and spatial distortions can be corrected by an adaptive optics (AO) system where deformable mirrors (DMs) and Shack-Hartmann wavefront sensors (WFSs) have been the preferred options to measure and apply the correction. However, photonic WFSs [4, 9] have recently been suggested to detect blind modes and non-common path aberrations (NCPAs), a limitation of pupil plane WFSs. Photonic wavefront correctors, on the other hand, have been used in experiments for satellite-to-ground free-space optical (FSO) communication [1].

We propose a photonic integrated circuit (PIC) capable of coherently coupling the beamlets from the subapertures of a telescope pupil into an SMF. As shown in Fig. 1, the PIC has a square array of grating couplers used to inject the light from free space into the plane of single-mode waveguides in a silicon-on-insulator (SOI) chip. High-resistance metal overlays are used to heat sections of the waveguides and modulate their refractive index through the thermo-optic effect. By shifting the phases of the propagating modes, the channels can be coherently combined, and the collected light can be delivered to one output SMF. In an AO system, the phase corrector would act as a DM commanded by a controller that takes phase measurements from a WFS. Simulations and performance metrics calculations for this concept were presented earlier [3]. The optical setup used and proof-of-concept lab results are presented here for a device capable of correcting 2×2 subapertures.

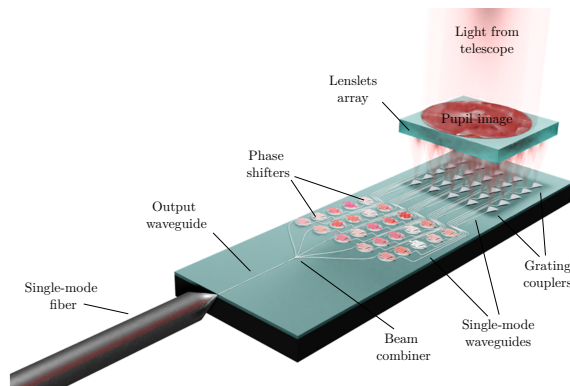


Figure 1. Concept of the photonic phase corrector. The distorted wavefront is focused by the lenslets array on the surface grating couplers. The coupled beamlets are shifted in phase and then combined into an SMF.

Photonic phase correctors have smaller footprints and require less power than classical correctors. Depending on the design, they could have much larger strokes and can be driven faster than deformable mirrors. In astronomical telescopes, the multiplexing advantage and flexibility of photonic phase correctors may be used in multi-object AO (MOAO) systems that feed narrow-band multi-object spectrographs (MOSs).

2. CIRCUIT DESIGN

Figure 2 shows micrographs of the components of the fabricated PIC. The design follows the standard rules of E-beam lithography foundries. The SOI chip has a 220 nm thick silicon layer on a $2 \mu\text{m}$ buried oxide (BOX) layer and a $725 \mu\text{m}$ handle Si wafer. A $2 \mu\text{m}$ oxide cladding (TOX) is deposited on top of the waveguides which also serves as protection from the environment. TiW metal traces are deposited on top of the TOX layer to create the heaters, whereas TiW/Al is used to make the contact pads. A third oxide layer is deposited to prevent the oxidation of the heaters where windows are opened over the pads to allow wiring.

The lines in the grating couplers are periodic with $1.5 \text{ lines}/\mu\text{m}$. An adiabatic tapered waveguide follows the grating and matches the coupled beam to the mode of the 450 nm single-mode waveguides on the chip. The phase shifters are coiled sections of the waveguides with the TiW metal layer deposited on top. The spiral geometry of the waveguides and the zigzag shape of the heater maximize the available stroke in phase. The subapertures are combined pair-wise with 2×1 combiners in a binary tree configuration. The output waveguide from the tree is coupled to a sub-wavelength grating that expands the mode size to $3 \mu\text{m}$ so that edge coupling is possible with a lensed SMF28 fiber.

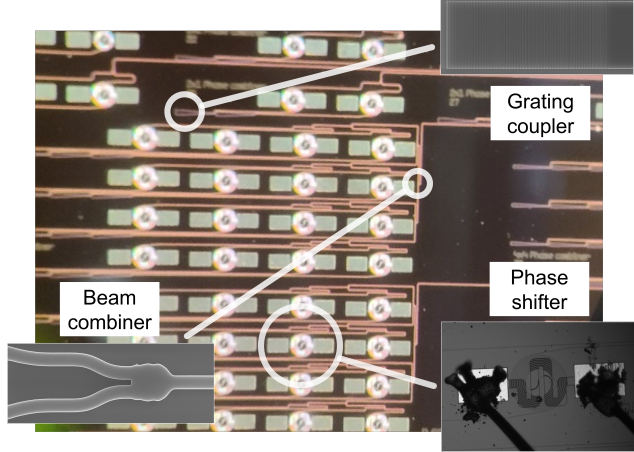


Figure 2. A top view of the circuit with micrographs of its components. The fabricated chip has multiple devices with different numbers of couplers (subapertures).

3. SIMULATION RESULTS

Detailed simulation results of the performance metrics and the operation range of the device were reported in [3]. We show here the expected performance of three of the PIC devices of different sizes. Figure 3 shows the Strehl ratio, defined as the peak intensity measured at the output of the PIC for a given distorted wavefront divided by the peak intensity measured for a planar wavefront. A sample of 100 Kolmogorov phase screens was used for the computation and a finite-difference time-domain (FDTD) package was used to propagate the distorted focal spots through a model of the device. Insertion and propagation losses were discussed in [3]. The overall throughput of the current first-generation device is expected to be $\sim 10\%$ due to insertion losses at the grating couplers, coupling losses at the output waveguide, and optical propagation losses in the PIC. The losses can be mitigated by improving the design of the gratings, switching to a SiN platform, optimizing the length of the waveguides in the PIC, and packaging the chip with the fiber aligned at the output. A theoretical throughput of 0.8 is possible. When Fig. 3 is read together with the throughput estimates and compared to the calculations of the efficiency of direct coupling into SMFs [5], one sees that a boost in efficiency by an order of magnitude is possible with an 8×8 device.

4. EXPERIMENTAL SETUP AND PRELIMINARY TESTS

The setup used to test the PIC is shown in Fig. 4. A single-mode fiber-coupled tunable laser is collimated with a doublet achromat and the polarization state of the beam is controlled in free space using a polarizer and a half-wave plate. A two-lens Keplerian telescope reduces the beam size to illuminate 2×2 lenslets in the MLA. An achromatic doublet pair is used to reimagine the focal plane of the MLA on the surface of the PIC.

The PIC is mounted on a 6-axis micropositioner so that the gratings can be aligned to the focal spots. A lensed tapered fiber is also mounted on a 6-axis micropositioner and aligned at the facet of the chip to edge-couple the light out of the waveguide. A phase screen that introduces atmospheric-like distortions in the beam may be inserted at a pupil plane conjugated to the plane of the MLA.

A microcontroller and a DAC circuitry drive currents into the wire-bonded heaters. A control loop can be closed using a photodiode to measure the output signal. Figure 5 shows the response of the output of the PIC to the sweeping of the voltage of one of the four heaters in a 2×2 device. The curve is the expected interference pattern where the output of one combiner in the binary tree is made to constructively (destructively) interfere with the remaining arms by shifting the phase with the applied voltage. A similar test is performed for all the gratings in the device under test to verify their functionality and establish their voltage response.

A stroke of 1.67 cycles/V ($V_\pi = 300$ nm) is observed. The voltage can be raised to about 20 V allowing strokes $> 50 \mu\text{m}$ optical path difference at the operating wavelength $\lambda = 1550$ nm. Since the parameter space of

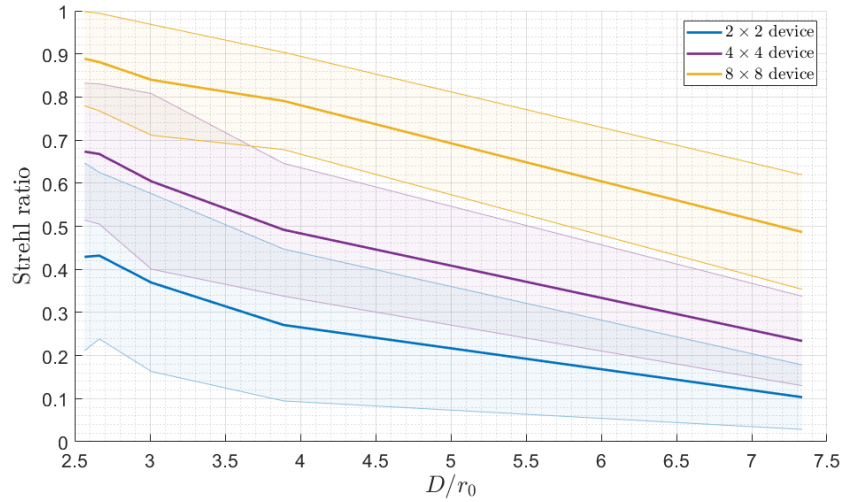


Figure 3. Dependence of the Strehl ratio (output peak intensity relative to the diffraction-limited case) on turbulence strength D/r_0 at 1550 for 2×2 , 4×4 , and 8×8 devices [3].

the 2×2 device is small enough, a gradient descent algorithm can be used to close the loop on a rotating phase screen without the need for wavefront sensing. However, a WFS will be necessary for larger devices correcting fast-changing wavefronts like those encountered in LEO-to-ground laser communication scenarios.

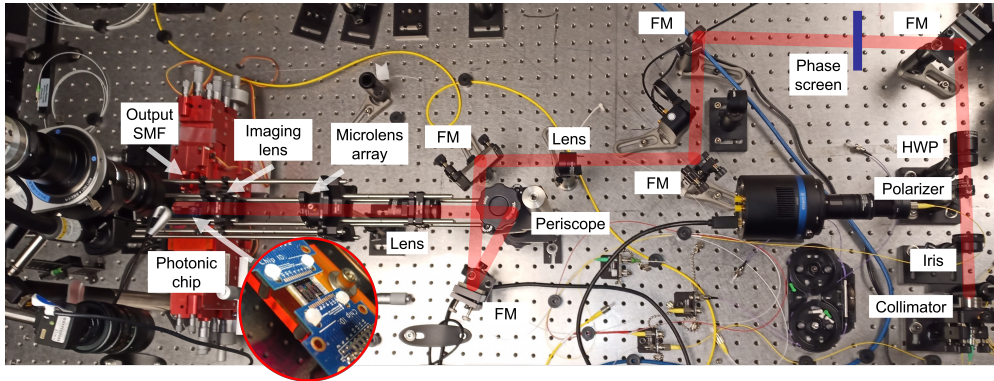


Figure 4. Optical setup for testing the phase shifters. The beam launched from an SMF is collimated and polarized on the right. The beam is distorted by a phase plate with Kolmogorov statistics. A Keplerian telescope resizes the pupil and a microlens array focuses the sub-apertures. A pair of achromats are used to reimage the spots on the chip surface. Micropositioners are used to align the chip and couple the light into an output fiber. FM: folding mirror. HWP: half-wave plate.

5. OUTLOOK

The photonic corrector presents a low-cost integrated solution for free-space optical communication applications. Optical ground stations have small apertures but need to deal with strong turbulence conditions since they track satellites very low in the sky and are usually built on sites with bad seeing. Classical AO solutions with mechanical deformable mirrors and bulk-optics wavefront sensors are expected to be too expensive and intricate for such applications. For H-band astronomical spectrographs, the starlight bandwidth is larger than that of the grating couplers (~ 40 nm FWHM), but due to the multiplexing advantage of PICs, one can envision a setup where multiple chips tuned at different central wavelengths are used to cover the entire H-band. The other

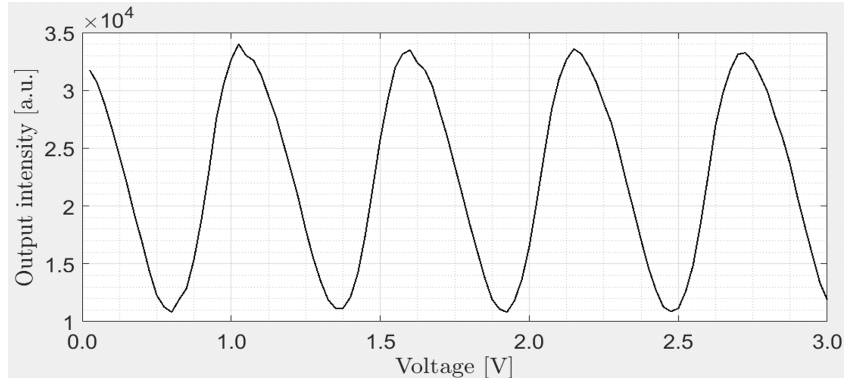


Figure 5. Electrical control of the total light intensity by local heating of optical delay waveguides. The interference pattern seen in the output signal is a result of shifting the phase of one waveguide relative to the others.

challenge to coherent combination is the relatively short coherence length ($\sim 20\mu\text{m}$) of the coupled polychromatic light. However, the stroke of the phase shifters can be engineered to be long enough, albeit at the cost of extra propagation loss. Furthermore, a multi-object spectrograph can be designed where each object is coupled to one PIC. The single-mode output waveguide also enables the use of photonic spectrographs [2] that can be fabricated on the same substrate, eliminating the out-coupling loss.

For small devices, e.g., 2×2 , a sensorless approach is used to correct the phases and close the loop. Optimization algorithms like stochastic gradient descent can find the co-phasing solution within the available coherence time if the array is small enough. For larger devices, we plan to implement either an external Shack-Hartmann WFS, where the interaction matrix can be synthetically calculated from simulations, or integrate Mach-Zehnder interferometers in the PIC as phase sensors.

The first-generation chip was meant as a proof of concept and only devices with 2×2 subapertures were wire-bonded and tested. The next-generation chips will have 8×8 devices, providing a PIC that can be used on-sky for a 50 cm telescope. The plan is also to package the chips to reduce the insertion losses and arrange the couplers in a hexagonal array for a better fill factor. Grating couplers with Si overlays and distributed Bragg reflectors (DBRs) will also be explored to enhance in-coupling.

ACKNOWLEDGMENTS

This work was supported by the High Throughput and Secure Networks Challenge Program at the National Research Council of Canada. We would also like to acknowledge CMC Microsystems for the provision of products and services that facilitated this research.

References

- [1] Antonin Billaud et al. “Turbulence Mitigation via Multi-Plane Light Conversion and Coherent Optical Combination on a 200 m and a 10 km Link”. In: *2022 IEEE International Conference on Space Optical Systems and Applications (ICSOS)*. Mar. 2022, pp. 85–92. DOI: [10.1109/ICSOS53063.2022.9749710](https://doi.org/10.1109/ICSOS53063.2022.9749710).
- [2] Ross Cheriton et al. “On-sky demonstration of astrophotonic fiber Fabry-Pérot correlation spectroscopy”. In: *Advances in Optical and Mechanical Technologies for Telescopes and Instrumentation V*. Vol. 12188. SPIE, Aug. 2022, pp. 1673–1680. DOI: [10.1117/12.2619244](https://doi.org/10.1117/12.2619244). URL: [https://www.spiedigitallibrary.org/conference-proceedings-of-spie/12188/121885F/On-sky-demonstration-of-astrophotonic-fiber-Fabry-P%*c3*%*a9*rot-correlation-spectroscopy/10.1117/12.2619244.full](https://www.spiedigitallibrary.org/conference-proceedings-of-spie/12188/121885F/On-sky-demonstration-of-astrophotonic-fiber-Fabry-P%c3%a9rot-correlation-spectroscopy/10.1117/12.2619244.full) (visited on 09/13/2023).
- [3] Momen Diab, Ross Cheriton, and Suresh Sivanandam. “Photonic phase correctors based on grating couplers: proof of concept simulations and preliminary performance metrics”. In: *Adaptive Optics Systems VIII*. Vol. 12185. SPIE, Aug. 2022, pp. 2720–2726. DOI: [10.1117/12.2642529](https://doi.org/10.1117/12.2642529).

- [4] Momen Diab and Stefano Minardi. “Modal analysis using photonic lanterns coupled to arrays of waveguides”. EN. In: *Optics Letters* 44.7 (Apr. 2019), pp. 1718–1721. ISSN: 1539-4794. DOI: [10.1364/OL.44.001718](https://doi.org/10.1364/OL.44.001718). URL: <https://www.osapublishing.org/ol/abstract.cfm?uri=ol-44-7-1718> (visited on 08/14/2020).
- [5] Momen Diab et al. “Starlight coupling through atmospheric turbulence into few-mode fibres and photonic lanterns in the presence of partial adaptive optics correction”. In: *Monthly Notices of the Royal Astronomical Society* 501.2 (Jan. 2021), pp. 1557–1567. ISSN: 0035-8711. DOI: [10.1093/mnras/staa3752](https://doi.org/10.1093/mnras/staa3752). URL: <https://doi.org/10.1093/mnras/staa3752> (visited on 01/15/2021).
- [6] S. C. Ellis et al. “Suppression of the near-infrared OH night-sky lines with fibre Bragg gratings – first results”. In: *Monthly Notices of the Royal Astronomical Society* 425.3 (Sept. 2012), pp. 1682–1695. ISSN: 0035-8711. DOI: [10.1111/j.1365-2966.2012.21602.x](https://doi.org/10.1111/j.1365-2966.2012.21602.x). URL: <https://doi.org/10.1111/j.1365-2966.2012.21602.x> (visited on 04/08/2021).
- [7] S. Gillessen et al. “GRAVITY: a four-telescope beam combiner instrument for the VLTI”. In: *Optical and Infrared Interferometry II*. Vol. 7734. International Society for Optics and Photonics, July 2010, 77340Y. DOI: [10.1117/12.856689](https://doi.org/10.1117/12.856689). (Visited on 05/16/2018).
- [8] Stefano Minardi et al. “Discrete beam combiners from astronomy to lasers”. In: *Integrated Optics: Devices, Materials, and Technologies XXIII*. Vol. 10921. SPIE, Mar. 2019, pp. 117–124. DOI: [10.1117/12.2512276](https://doi.org/10.1117/12.2512276). URL: <https://www.spiedigitallibrary.org/conference-proceedings-of-spie/10921/1092110/Discrete-beam-combiners-from-astronomy-to-lasers/10.1117/12.2512276.full> (visited on 05/11/2022).
- [9] Barnaby R. M. Norris et al. “An all-photonic focal-plane wavefront sensor”. en. In: *Nature Communications* 11.1 (Oct. 2020). Number: 1 Publisher: Nature Publishing Group, p. 5335. ISSN: 2041-1723. DOI: [10.1038/s41467-020-19117-w](https://doi.org/10.1038/s41467-020-19117-w). URL: <https://www.nature.com/articles/s41467-020-19117-w> (visited on 05/05/2021).
- [10] Martin M. Roth et al. “Astrophotonics: photonic integrated circuits for astronomical instrumentation”. In: *Integrated Optics: Devices, Materials, and Technologies XXVII*. Vol. 12424. SPIE, Mar. 2023, pp. 44–59. DOI: [10.1117/12.2655630](https://doi.org/10.1117/12.2655630). URL: <https://www.spiedigitallibrary.org/conference-proceedings-of-spie/12424/124240B/Astrophotonics-photonic-integrated-circuits-for-astronomical-instrumentation/10.1117/12.2655630.full> (visited on 10/14/2023).
- [11] Andreas Stoll et al. “Integrated échelle gratings for astrophotonics”. In: *Advances in Optical Astronomical Instrumentation 2019*. Vol. 11203. International Society for Optics and Photonics, Jan. 2020, 112030Z. DOI: [10.1117/12.2541554](https://doi.org/10.1117/12.2541554). URL: <https://www.spiedigitallibrary.org/conference-proceedings-of-spie/11203/112030Z/Integrated-echelle-gratings-for-astrophotonics/10.1117/12.2541554.short> (visited on 11/30/2020).